

Artificial neural networks applied to quantitative elemental analysis of organic material using PIXE

R. Correa^a, M.A. Chesta^{b,*}, J.R. Morales^c, M.I. Dinator^c, I. Requena^d, I. Vila^e

^a Universidad Tecnológica Metropolitana, Departamento de Física, Av. José Pedro Alessandri 1242, Ñuñoa, Santiago, Chile

^b Universidad Nacional de Córdoba, Facultad de Matemática, Astronomía y Física, Medina Allende s/n Ciudad Universitaria, 5000 Córdoba, Argentina

^c Universidad de Chile, Facultad de Ciencias, Departamento de Física, Las Palmeras 3425, Ñuñoa, Santiago, Chile

^d Universidad de Granada, Departamento de Ciencias de la Computación e Inteligencia Artificial,

Daniel Saucedo Aranda s/n, 18071 Granada, Spain

^e Universidad de Chile, Facultad de Ciencias, Departamento de Ecología, Las Palmeras 3425, Ñuñoa, Santiago, Chile

Received 23 December 2005; received in revised form 13 April 2006

Available online 16 June 2006

Abstract

An artificial neural network (ANN) has been trained with real-sample PIXE (particle X-ray induced emission) spectra of organic substances. Following the training stage ANN was applied to a subset of similar samples thus obtaining the elemental concentrations in muscle, liver and gills of *Cyprinus carpio*. Concentrations obtained with the ANN method are in full agreement with results from one standard analytical procedure, showing the high potentiality of ANN in PIXE quantitative analyses.

© 2006 Elsevier B.V. All rights reserved.

PACS: 29.85.+c; 87.64.Gb; 07.05.Tp

Keywords: Artificial neural networks; PIXE

1. Introduction

Developments from artificial intelligence like artificial neural networks, ANN, can be regarded as an engineering procedure emulating the human brain activity. It can be defined as a set of non-linear and non-stationary interconnection of elemental processes able to carry out at least one of the following functions: training, remembrance and generalization, or, abstraction of substantial properties. The fundamentals of the ANN technique have been described elsewhere [1,2] and several commercial and free codes are accessible nowadays.

Applications of ANN to atomic and nuclear physics has increased during the last two decades [3–13], mainly in problems related to nuclear reactors. The most used paradigms in artificial intelligence applications to nuclear science and particle physics are the expert system, genetic algorithms, fuzzy system, neural networks and hybrid system. Some applications to α , γ and X-ray spectra have been reported in the last decade [14–17]. Further application of ANN in other cases where strong non-linear effects are present like in the spectral analyses generated in analytical techniques like PIXE [18,19] and XRF (X-ray fluorescence) [20,21] are scarce and in BIXE spectra (beta induced X-ray emissions) remain unexplored [22,23]. In [24,25] a review of applications of ANN and its potentialities in atomic and nuclear physics is shown.

A case where the potentialities of ANN seem to be most convenient is in the repetitive analysis of many spectra presenting similar patterns with specific differences. A typical

* Corresponding author. Tel.: +54 351 4334052; fax: +54 351 4334054.

E-mail addresses: rcorrea@utem.cl (R. Correa), chesta@famaf.unc.edu.ar (M.A. Chesta), rmorales@uchile.cl (J.R. Morales), mdinator@uchile.cl (M.I. Dinator), requena@decsai.ugr.es (I. Requena), limnolog@uchile.cl (I. Vila).

case is presented in the elemental analysis of samples of unknown composition using energy dispersive XRF spectroscopy. Their respective spectra present peaks of known energy but different intensities containing information required to the evaluation of the elemental concentrations in each sample.

PIXE is a well established analytical method that allows the determination of concentrations in the range of mg/kg [26,27]. One of the factors that define the quality of the analysis is the ability to determine the correct amount of counts in each peak. Usually this is accomplished by the use of some reliable computer code, like AXIL [28].

Additional inputs of the proper physical parameters involved in the irradiation like beam intensity, detector efficiency, geometrical parameters, etc., permit the determination of the elemental concentrations.

The purpose of this work has been to take advantage of the non-linear properties and the neural network ability to learn and generalize together with its fast response. Samples of fish tissues were irradiated with protons to determine their elemental concentrations as part of a study of metal bioaccumulation by fishes. Several PIXE spectra were obtained from muscle, liver and gills samples of *Cyprinus Carpio*. A part of the samples set was analyzed by the standard method and later used to train the ANN for further calculations. Without assumptions about the distribution of data it was possible to detect elements (P, S, K, Ca, Fe, Zn) and determine their concentration in these organic samples obtained from fishes captured in Rapel Lake in Chile.

2. Analysis

The analysis was performed in two phases. First, one in which PIXE spectra were used to train the ANN and a second one in which the application of ANN independently produced results that were compared with those obtained by standard methodology.

PIXE spectra from muscle, liver and gills samples were used together with proper experimental data like average beam intensity, irradiation times, target masses, plus cross-sections values and detection system sensitivity, to determine elemental concentrations. As mentioned above, the amount of counts in each peak is currently used to determine the elemental concentration. Here, a slightly different approach has been used based on the fact that ANN application disregards additive constants. Then considering the observation that the background contribution at the peak is rather constant for equal irradiation times, the use of the maximum value at the peak channel as an input in ANN calculations, simplifies data handling and provides equivalent results as those obtained when the full area is used. These values and the already known concentrations were given as an input and output data respectively in the ANN training phase. Fig. 1 shows the flux diagram followed in each phase.

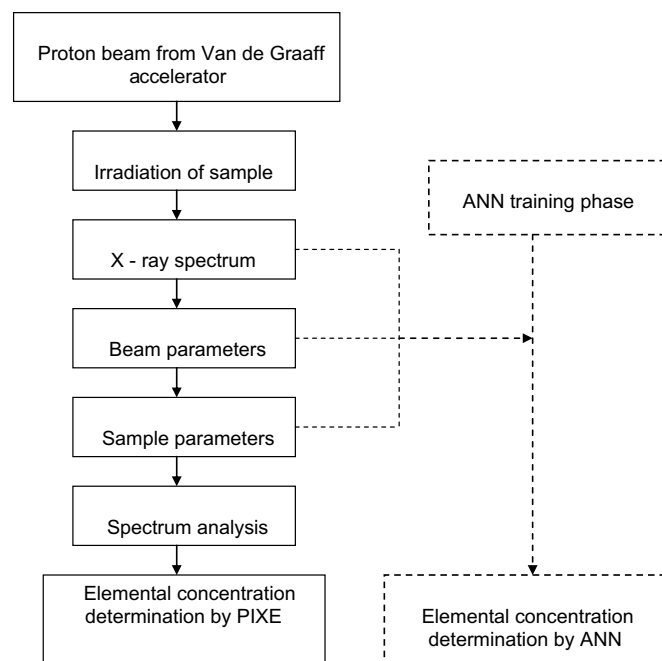


Fig. 1. Flux diagram showing the relationship between ANN inputs and the classical PIXE experimental steps.

2.1. PIXE analysis

The PIXE applications were performed at the Center for Experimental Physics, Faculty of Sciences, University of Chile, using the KN 3750 Van de Graaff electrostatic accelerator. Twenty one biological samples from a (*C. Carpio*) fish were prepared by digestion with HNO_3 and deposited on $8.4 \mu\text{m}$ thickness Kapton films for later irradiation with a 2.0 MeV proton beam. The X-ray photons emitted from the samples were detected by a Si(Li) detector (FWHM = 180 eV at 5.9 keV) coupled to conventional electronic units and MCA. The detector was placed at 90° angle with respect to the incident beam. A typical spectrum from a liver sample is shown in Fig. 2, where the characteristic $\text{K}\alpha$ and $\text{K}\beta$ peaks appear over the continuous

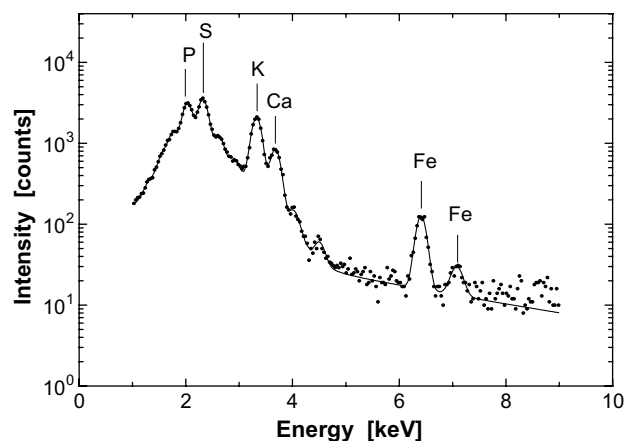


Fig. 2. Typical PIXE spectrum of a liver sample from fish *C. carpio*, using 2.0 MeV protons. The solid line is a fit given by AXIL.

background. These X-ray spectra were analyzed using AXIL [28] code provided by IAEA, obtaining the net number of counts in each peak for later use. Certified foils from Micromatter for a number of elements are currently used for quality assurance.

In order to get the elemental concentration it is required to know the absolute sensitivity of the spectroscopic system, which can be expressed in terms of fundamental parameters as:

$$J(E) = \frac{N_0}{e \cdot A} \cdot \sigma_K(Z) \cdot \omega_K(Z) \cdot g_{K_i}(Z) \cdot \varepsilon(E), \quad (1)$$

where σ_K (cm^2), ω_K and g_{K_i} ($i = \alpha, \beta$) are, respectively, K-shell ionization cross-section, fluorescence yield and line fraction. $\varepsilon(E)$ is the absolute efficiency function of the detector, N_0 is the Avogadro number, e (C) is the elemental charge and A is the atomic mass of the Z -element.

Here the sensitivity was determined by a set of N -standard thin film targets from Micromatter irradiated under similar conditions as the biological ones [29]. Certified samples of Al, SiO, CuS, KCl, CaF₂, Cr, Fe, ZnTe and CdSe were used to obtain the efficiency parameter J expressed per unit of charge and per unit of mass surface density in the energy region of interest (i.e. 2–8 keV). The $J(E)$ fitting function was obtained from the N -standard samples J_l ($l = 1, 2, \dots, N$) through the equation.

$$J_l = J(E_{K_i}^l) = \frac{I_{\text{st}}^l(E_{K_i}^l)}{Q^l \cdot m_{\text{st}}^l}, \quad (2)$$

where I_{st}^l represents the net number of counts in the K_i peak ($i = \alpha, \beta$), Q^l is the collected charge at the Faraday cup and m_{st}^l the mass per unit area. The fitted function $J(E)$ is shown in Fig. 3.

The concentration of the Z -element, C_Z , defined as the quotient between the elemental mass and the total mass of the sample, was calculated using the following equation:

$$C_Z = \frac{I_Z(E_{K_i})}{M \cdot Q \cdot J(E_{K_i})}, \quad (3)$$

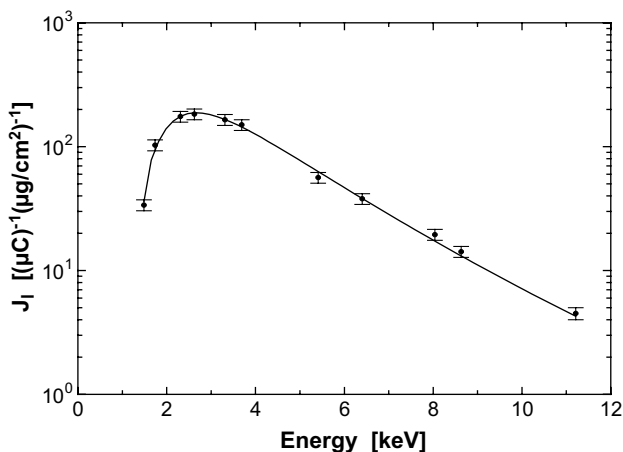


Fig. 3. K_{α} sensitivity curve obtained using thin film standards from Micromatter. The solid line is a parametric fit, from [30].

where I_Z , Q and M have the same meanings as before but now in reference to the sample and $J(E)$ ($\text{g}^{-1} \text{cm}^2 \text{C}^{-1}$) was defined above.

The results obtained by the PIXE procedure are considered as “expected concentrations” when ANN are used.

2.2. ANN analysis

A feed-forward ANN has been used in the learning phase, directly from concentration data obtained in real time. The ANN was trained with the well known back propagation algorithm in order to learn first and then reproduce the process in order to obtain the concentration of certain chemical elements in some organic samples. The neural network feeds with input parameters like:

- The proton beam intensity impinging the sample.
- Mass and surface area of the sample.
- Spectral information of the detected X-ray.

For each element, an ANN with three layers (input, hidden, output) was used to generate the mapping of the p -input parameters (in this work $p = 4$, indicated in (a), (b) and (c) above and specified below) to the q -output parameters, here represented by the concentration of the element in the sample ($q = 1$). The mapping is carried out using the weights of the neuron connections, computed in the supervised training process.

For training, the method for least square error back propagation, the most often used supervised learning algorithm, was used. Supervised learning means that for each example, both the input and the expected output (the output that ANN must produce) are known; so, training the ANN means that the computed outputs must be the closest to the expected outputs for each example. From a general point of view we consider a neural network with p -inputs, one hidden layer with L -neurons ($L = 4$ in this case) and one output node. The value of the error E_k on an input/output training pattern (x^k, y^k) is defined by:

$$E_k = 1/2(y^k - O^k)^2, \quad (4)$$

where O^k is the computed output generated when the k th input vector $x^k = (x_1^k \dots x_p^k)$ is presented to the network and the transformation is conducted by the transfer sigmoid function and where y^k is the expected value for the output corresponding to input x^k .

$$O^k = (1 + \exp(-Wh^k))^{-1}, \quad (5)$$

where $h^k = (h_1^k \dots h_L^k)$ is the output vector of the hidden layer and W is the weight vector of the output neuron:

$$h_l^k = \left(1 + \exp\left(-\sum w_l x^k\right)\right)^{-1}, \quad (6)$$

and where w_l denotes the weight vector of the l th hidden neuron, ($l = 1, \dots, L$); and the overall measure of the error is

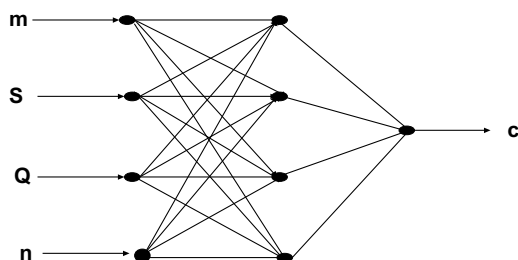


Fig. 4. NN topology for application with four inputs (m, S, Q, n), four hidden neurons and one output neuron (concentration – C).

$$E = \sum E_k. \quad (7)$$

The rule for changing weights following presentation of input/output pair k is given by the gradient descent method, i.e. the quadratic error function is minimized by using the iteration process.

After the training phase was completed, a test procedure to verify that the neural net effectively did learn the lessons was performed.

To determine the concentrations of the elements: P, S, K, Ca, Fe and Zn in the sample, a three-layers feed-forward ANNs, with 4 inputs, 4 hidden neuron and 1 output (4-4-1), was used for each element. The inputs, m, S, Q and n (see Fig. 4) are, respectively, the mass and area of the sample, the collected charge and the number of counts in the maximum of the K_α peak in the considered element.

For each of the 21 available samples, we consider five values for the ANN training, four (m, S, Q, n) as input training (x^k in Eqs. (4)–(7)), and one (elemental concentration) as expected output (y^k in the equations). To train the ANN, first the initial weights are fixed in a random way. Then each sample (the 4 input values) is introduced in the ANN, which compute the output (O^k in the above equations), it is say, the actual concentration value. This value is compared with expected concentration value and according to the error, the weights are modified so that both values (computed concentration and expected concentration) become the closest possible.

Usually the training set is defined experimentally. In this case due to the rather low number of available samples, according to the experience of the authors a training set of 18 spectra randomly selected and a testing set of three spectra were used in each ANN. Results confirmed that this selection was adequate.

An ANN for each the six considered elements, with similar topology, was trained in an independent manner and the sigmoid activation function was used in the hidden and output layers. The topology and the parameters used (learning rate, momentum, error value, etc.) were obtained in an experimental way.

3. Results and discussion

Without missing generality in this ANN application only the six major elements, P, S, K, Ca, Fe and Zn

observed in the spectra were considered. Trace elements, although important for other studies, were not statistically useful for the present purpose. Elemental concentrations were calculated by standard PIXE methodology in the way described above. These results were considered as “expected concentrations”. As for PIXE uncertainties, overall values ranged between 6% and 10%. The major source of error was the determination of the total mass surface density in each sample. This was due to the type of the materials analysed, fish tissue, which turn to form non-uniform layers on the backing Mylar foil.

In turns, a feed-forward neural network, with definite topology was independently trained in parallel with the backward error propagator to determine the elemental concentrations of interest in the organic samples of this study. The same six major elements common to the three type of samples, gill, liver and muscle, were considered.

A total of 21 spectra (seven gills, seven liver, seven muscle) provided 21 peaks for each element. Of these, 18 spectra were randomly selected (the same spectra for each element) and used in training the network and three were used in testing it. All training cases were learned correctly by each of the six neural networks.

Only for one test case (corresponding to element Zn) the ANN predictions are out of one standard deviation from the PIXE results. Bioaccumulation of Zn in muscle tissue is low and its concentration is close to the detection limit for this element and therefore larger uncertainties are expected affecting the ANN predictions. The agreement is illustrated in Fig. 5, where concentrations are shown for each element in samples of gill, liver and muscle, from the test set.

To asses the goodness of the ANN method in providing concentrations values, a comparison with PIXE results was done and is shown in Fig. 6. A linear regression calculation for results from all elements, in the test and training sets, was performed. Correlations factor, r^2 , of 0.86 and 0.99 were obtained for the test and training sets, respectively.

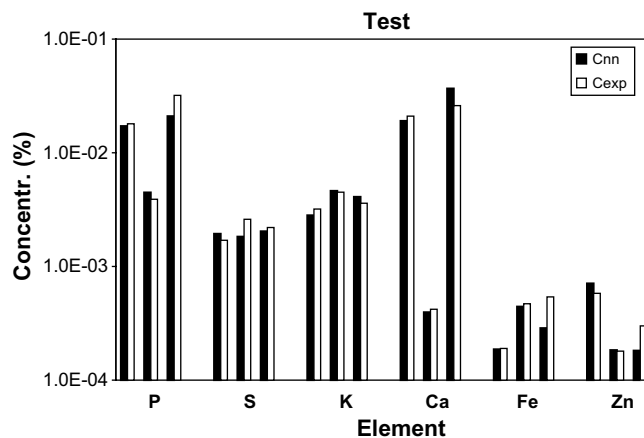


Fig. 5. Elemental concentration obtained from the three samples of the test set using ANN (C_{NN}) and PIXE (C_{exp}), are shown for gill, liver and muscle respectively for each element.

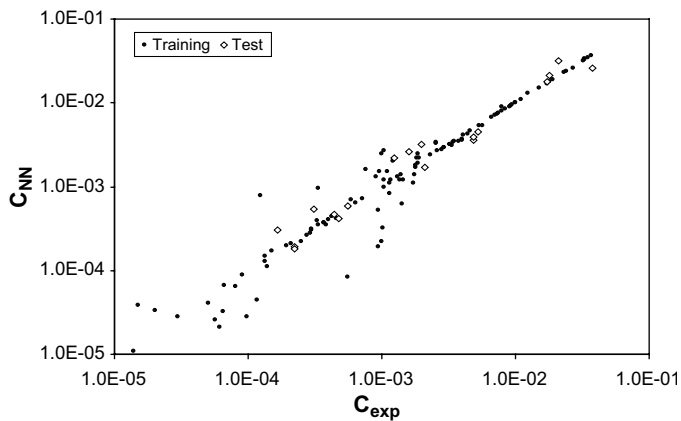


Fig. 6. The predicted concentrations from ANN (C_{NN}) as compared with PIXE (C_{exp}) concentrations.

4. Conclusions

The main purpose of this work was to explore the application of ANN for a fast analysis of PIXE spectra in a study of bioaccumulation of metals. It has been proved that this methodology provides results as good as those obtained by one of the already accepted methods. Even though the number of cases was rather limited, the decision to use independent neuronal topologies for each element working in parallel, provided reliable results. Surely, the experimental results would be improved with a greater number of cases to use as training and test sets, but with the 21 available cases, the results are enough good. So, the use of ANN as a reasonable alternative for the elemental concentration determination in PIXE procedure, has been established. In addition, this ANN application proved to be fast enough as to predict that the analysis of a great number of samples can be accomplished in few minutes, avoiding the direct participation of the analyst in each one. Once the ANN has been trained, its use become fast thus permitting the automation of PIXE spectra analysis and reducing costs and time.

Acknowledgements

We acknowledge the technical assistance of Mr. S. Cancino and Mr. H.O. Riquelme in the operation of the Van de Graaff accelerator. The dedication of Ms. P. Auriol in sample preparation is appreciated. Financial support from the Center for Experimental Physics, Faculty of Science, University of Chile is recognized.

References

- [1] S. Haykin, *Neural Networks: A Comprehensive Foundation*, Macmillan, College Publishing, New York, 1994.
- [2] R. Rojas, *Neural Networks. A Systematic Introduction*, Springer-Verlag, 1996.
- [3] K. Brudzewski, S. Osowski, *Sens. Actuators B* 55 (1999) 38.
- [4] B. Denby, *Nucl. Instr. and Meth. A* 389 (1997) 8.
- [5] B. Denby, *Comp. Phys. Com.* 119 (1999) 219.
- [6] L. Dolmatova, V. Teshistakov, C. Ruckebusch, N. Dupuy, J.P. Huvenne, *J. Chem. Inf. Comput. Sci.* 39 (1999) 1027.
- [7] D. Horn, *Nucl. Instr. and Meth. A* 389 (1997) 381.
- [8] C.C. Ku, K.Y. Lee, R.M. Edwards, *Trans. Am. Nucl. Soc.* 63 (1991) 114.
- [9] C.C. Ku, K.Y. Lee, R.M. Edwards, *IEEE Trans. Nucl. Sci.* 30 (6) (1992) 2298.
- [10] M. Marseguerra, S. Minoggio, A. Rossi, E. Zio, *Prog. Nucl. Eng.* 27 (4) (1992) 297.
- [11] U. Muller, *Nucl. Instr. and Meth. A* 502 (2003) 811.
- [12] J.J. Ortiz, J.L. Montes, I. Requena, R. Perusquía, *Ann. Nucl. Energy* 31 (16) (2004) 1939.
- [13] R.E. Uhrig, *Nucl. Saf.* 32 (1) (1991) 68.
- [14] C. Citterio, A. Pelgotti, V. Piuri, L. Roca, *IEEE Trans. Neural Networks* 10 (4) (1999) 725.
- [15] L.J. Kangas, G.L. Troyer, P.E. Keller, S. Hashem, R.T. Kouzes, in: *Proc. of IEEE Nuclear Science Symp. and Medical Imaging Conf.*, Norfolk, USA, 1994, p. 346.
- [16] P.E. Keller, R.T. Kouzes, in: *Proc. of IEEE Nuclear Science Symp. and Medical Imaging Conf.*, Norfolk, USA, 1994, p. 341.
- [17] J. Zimmermann, C. Kiesling, P. Holl, *Nucl. Instr. and Meth. A* 502 (2003) 507.
- [18] S. Iwasaki, H. Fukuda, M. Kitamura, *Int. J. PIXE* 3 (1993) 267.
- [19] J. Wang, P. Guo, X. Li, J. Zhu, T. Reinert, J. Heitmann, D. Spermann, J. Vogt, R.H. Flagmeyer, T. Butz, *Nucl. Instr. and Meth. B* 161–163 (2000) 830.
- [20] I. Facchin, C. Mello, M. Bueno, R. Poppi, *X-ray Spectrom.* 28 (1999) 173.
- [21] E.A. Hernández-Caraballo, L.M. Marco-Parra, *Spectrochim. Acta B* 58 (2003) 205.
- [22] M.A. Chesta, T.S. Plivelic, R.T. Mainardi, *Nucl. Instr. and Meth. B* 145 (1998) 459.
- [23] R.T. Mainardi, M.A. Chesta, M. Caffaro, *X-ray Spectrom.* 33 (2004) 112.
- [24] R. Correa, I. Requena, in: *Proc. of ESTYLF'04*, Jaen, Spain, 2004, p. 25.
- [25] R. Correa, I. Requena, in: *Proc. of IFSA'05*, Beijing, China, 2005, p. 346.
- [26] J.R. Morales, M.I. Dinator, *J. Radioanal. Nucl. Chem.* 140 (1) (1990) 133.
- [27] J.R. Morales, M.I. Dinator, F. Llama, J. Saavedra, F. Fallabella, *J. Radioanal. Nucl. Chem.* V 187 (1) (1994) 79.
- [28] B. Vekemans, K. Janssens, L. Vincze, F. Adams, P. Van Espen, *X-ray Spectrom.* 23 (1994) 278.
- [29] S.A.E. Johansson, J.L. Campbell, *A Novel Technique for Elemental Analysis*, John Wiley and Sons, 1988, p. 66.
- [30] V. Delgado Martinez, R.T. Mainardi, R.A. Barrea, C. Martinez Hidalgo, P.A. Derosa, M. Marco Arbolí, *X-ray Spectrom.* 27 (1998) 321.